In Vivo Imaging of Extraction Fraction of Low Molecular Weight MR Contrast Agents and Perfusion Rate in Rodent Tumors

David A. Kovar, Marta Z. Lewis, Jonathan N. River, Martin J. Lipton, Gregory S. Karczmar

Tissue uptake of a fully extractable MR detectable tracer, deuterated water (D_2O), was compared with that of a less extractable contrast agent, Gadolinium-DTPA-dimeglumine (Gd-DTPA), in rodent tumor and muscle tissue. This dual tracer method allowed calculation of relative (to muscle) tissue perfusion and extraction fraction of Gd-DTPA in each image pixel *in vivo*. Solutions of Gd-DTPA and D_2O were injected intravenously into Fisher female rats ($n = 9$) with R3230 mammary adenocarcinomas implanted in the hind limb. Perfusion rate was approximately two times greater ($P < 0.005$ by paired t test) in tumor than in muscle. Gd-DTPA extraction fraction at the interface between tumor and muscle was 2.0 times the extraction fraction in normal muscle ($P < 0.005$ by paired t test). Extraction fraction at the tumor center was 1.6 times the extraction fraction in muscle ($P < 0.01$ by paired t test). High extraction fraction of Gd-DTPA correlated with high capillary permeability determined from Evans Blue staining. Low molecular weight Gd-DTPA derivatives are widely used in clinical practice, and their extraction fractions are crucial determinants of image contrast during the first few passes of the contrast agent bolus. Therefore spatially resolved measurements of contrast agent extraction fractions obtained *in vivo* have significant clinical utility. The data demonstrate that extraction of low molecular weight tracers is sensitive to increased permeability in tumor vasculature and that this increased permeability can be imaged.

Key words: perfusion rate; extraction fraction; magnetic resonance; Gd-DTPA.

INTRODUCTION

Recent studies of tumor vascularity in biopsy samples obtained from human mammary tumors suggest that characterization of tumor vascular density and permeability allows accurate grading of mammary tumors and can guide treatment of patients (1–7). It would be beneficial if tumor vasculature could be accurately characterized using a noninvasive imaging method. This may be possible using MR contrast agents. Microstructural characteristics of vasculature can be inferred from contrast agent dynamics, even when image resolution is insufficient to show the microstructure explicitly. The tissue uptake kinetics of partially extractable contrast agents are dependent on the product of tissue perfusion and extraction fraction. The rate of tissue perfusion is dependent on vessel density (3) and the extraction fraction is a good indicator of capillary permeability (although the linear velocity of blood flow is also important). Therefore measurements of contrast agent tissue concentration as a function of time are sensitive to both capillary density and permeability. However, conventional methods cannot distinguish the effects of capillary density and capillary permeability on the rate of contrast agent uptake. This is especially true of low molecular weight contrast agents, for which the rate of transport across capillary walls is similar to the rate of delivery via tissue perfusion. We demonstrate here that perfusion rate and extraction from capillaries into the extravascular compartment can be distinguished by measuring the kinetics of uptake of partially extractable (i.e., Gd-DTPA-dimeglumine) and fully extractable (such as D_2O) tracers in combination.

Contrast agents leave capillaries primarily through gaps or pores in the capillary endothelium (8, 9), thus making the extraction fraction sensitive to the presence of irregularly formed capillary endothelia, which are common in tumors, particularly in areas of neo-vasculature. The use of smaller molecules to evaluate capillary permeability has several advantages: 1) only low molecular weight MR contrast agents are currently approved for human use in the United States, and they are better tolerated than high molecular weight compounds; 2) low molecular weight molecules may be sensitive to small early changes in capillary permeability; and 3) low molecular weight contrast agents are rapidly extracted into tissue in high concentrations. Gd-DTPA derivatives, in particular, are relatively nontoxic and can be detected with high SNR. In normal tissue outside of the brain, the Gd-DTPA-dimeglumine extraction fraction is ~0.45 (10). Thus tissue pathology typically would be indicated by extraction fractions ranging from 0.50 to 1.0.

The extraction fraction of Gd-DTPA derivatives can be measured by comparing their uptake to that of deuterated water (D_2O). The rate of tissue uptake of D_2O following intravenous bolus injection is widely used to measure perfusion rate (in milliliters/100 g of tissue × minutes) because it is approximately fully extracted ($E = 1.0$) from the capillary bed during a single passage (i.e., during the mean transit time). A large body of work (e.g., 11–14) validates the use of magnetic resonance detection of D_2O uptake for accurate perfusion measurements. Kim and

MRM 38:259–268 (1997)

From the Department of Radiology, University of Chicago, Chicago, Illinois.

Address correspondence to: Gregory S. Karczmar, Ph.D., Department of Radiology-MC2026, University of Chicago, 5841 South Maryland Avenue, Chicago, IL 60637.

Received May 20, 1996; revised February 3, 1997; accepted February 4, 1997.

This work was supported in part by the American Cancer Society, NIH (USPHS: 5 R29 CA52008) and Nycomed Inc. The Magnetic Resonance Imaging and Spectroscopy facility was constructed with the help of an NIH Shared Instrumentation grant and support from the General Electric Corporation.

0740-3194/97 $3.00

Ackerman *et al.* measured perfusion rates in rodent kidney, liver, brain, muscle and tumor (11, 13–15). Later work incorporated MR imaging of D_2O so that spatial heterogeneity of perfusion could be detected (16, 17). Besides use of D_2O, perfusion measurements based on the rate of uptake of tritiated water gave results similar to those obtained with microspheres (18).

To date, imaging studies of capillary permeability have been based on the use of macromolecular agents such as Gd-DTPA-albumin (19–24). Leakage of macromolecules across capillary walls provides a good measure of permeability and can be used to identify abnormal tumor vasculature (19–24). Extraction from vasculature of these macromolecules in normal tissue is close to zero, while in many tumors extraction is small but measurable. Thus, any accumulation of contrast agent in tissue can be taken as an indication of the abnormal capillary leakiness characteristic of tumors (25, 26). However, macromolecular agents have a number of disadvantages. They are not currently approved for routine use in patients in the United States. Permeability to these agents, even in tumor vasculature, is small, and to achieve adequate signal-to-noise ratio, leakage from the vasculature must often be detected over hours, or in some cases days (25–27). Tissue extraction of macromolecules requires relatively large pores in capillary walls and thus may be insensitive to subtle changes in capillary permeability. For these reasons, low molecular weight contrast agents may have advantages as indicators of capillary permeability.

In vivo measurements of contrast agent extraction fraction are necessary for interpretation of MR contrast enhanced images, particularly as rapid imaging of contrast agent uptake becomes increasingly common. Extraction fraction is a critical determinant of signal intensity at short times after the injection of contrast agents, and may vary considerably as a function of tissue type. However, to date, few measurements of the extraction fractions of low molecular weight contrast agents have been reported, and there have been no spatially resolved measurements of extraction fractions *in vivo*. Here, we demonstrate a simple method for obtaining this information.

METHODS

Tumor Transplantation

R3230AC mammary adenocarcinomas were grown subcutaneously in the hind limbs of female Fisher 344 rats. Tumors were studied after 3 weeks when they were 7–12 mm in diameter. The tumors are relatively non-metastatic and are not significantly necrotic in this size range. These tumors originally occurred spontaneously and are species-specific for Fisher 344 rats (28). Initial tumor cells were obtained from Biomeasure Corporation (Frederick, MD). The tumor line was propagated *in vivo*.

Anesthesia and Preparation

Animals were anesthetized by continuous intraperitoneally administration of ketamine (5 mg/100 g/h) and rompun (0.1 mg/100 g/h). The temperature of the animals was controlled by using a warm water blanket. In addition, the magnet bore was flushed continuously with warm air. To minimize motion artifacts, rats were secured to an acrylic plastic board using elastic webbing and Velcro (Manchester, NH). The tumor-bearing leg was immobilized horizontally, placed in the detector coil along with a water phantom and secured with tape. Blood pressure was measured continuously during MR studies using a catheter (PE-50) implanted in the femoral artery attached to a pressure transducer and a Tektronix monitor (Beaverton, OR). Mean arterial blood pressure under control conditions was between 100 and 140 mmHg. Animal temperature was measured continuously using a rectal thermometer (Fisher Scientific, Pittsburgh, PA) and was kept between 36°C and 38°C.

Coils

Signals were excited and detected by a dual coil system placed directly around the tumor-bearing leg. A 2.5-cm inner-diameter saddle coil tuned to the D_2O frequency was nested inside a 3.5-cm inner-diameter low pass birdcage coil (29, 30) tuned to the proton frequency. The loaded Q values for the saddle coil and the birdcage coil were 60 and 40, respectively. The birdcage coil had eight arms with seven 5.6 pF fixed capacitors and two 1–30 pF variable capacitors. The coils were oriented so that their RF fields were approximately orthogonal. Due to this orthogonality, as well as the large frequency difference between the two coils, there was minimal coupling. This was demonstrated by the fact that negligible tuning changes and 90° pulse length changes were caused in either coil by the other coil. The loaded 90° pulse lengths were 60 μs for the D_2O coil and 40 μs for the proton coil at 100 watts.

The birdcage coil provided an extremely homogeneous radio frequency (RF) field with variations of no more than 5% up to 1 mm from the edges of the cylinder. Thus, the 90° pulse length was constant across the field of view. There was some inhomogeneity of pulse angle at the edges of the slices since slice profiles were not perfect. However, since very thick (1.3-cm slices) were used to facilitate comparisons of proton and D_2O data, the volumes of the edge regions were negligible compared with that of the central region where the pulse angle was constant. This allowed accurate quantitation of the contrast agent based on measurement of changes in T_1. The field produced by the saddle coil was somewhat less homogeneous and data were analyzed to correct for this source of inhomogeneity (Eq. [5]).

Histology and Evans Blue

To correlate histological and MR data, the tumor was marked with a dark tattoo along the line of the slice imaged by MR. Histology provided an estimate of the degree of necrosis in the slice (from Hematoxylin and Eosin). Tumors were included in the data analysis *only* if necrosis was found in less than 10% of the surface area of the slice.

Evans Blue staining was performed. Evans Blue binds to circulating albumin to produce a macromolecular vital dye which escapes only from "leaky" capillaries. Therefore extraction of Evans Blue through capillary walls into extravascular spaces is an index of capillary permeability. The Evans Blue solution was injected via an intrave-

nous jugular catheter. Evans Blue studies were performed on the same tumor line, but in many cases were *not* performed on the tumors studied by MR.

MR Measurement Protocol

For 3 days before the MR experiment, D_2O was injected intraperitonneally (1.0 ml/day). This was done to provide signal for calibration measurements (see below). Approximately 30 min were required to prepare and position the animal in the magnet. Approximately 2.5 h were required for the entire experiment (i.e., preparation, D_2O and Gd-DTPA dimeglumine injections, and image acquisition). Our data (see Results and refs. 31, 32) indicate that blood flow and metabolism are stable over this time period under ketamine-rompun anesthesia.

MR data were acquired at 4.7 Tesla using a GE-Bruker Omega operating system. The proton coil was initially connected and used for positioning and shimming. The deuterium coil was then connected and the deuterium preamplifier was manually retuned. A deuterium density image was acquired under fully relaxed conditions (TR = 3 s with a 45° pulse angle) with TE minimized (4.5 ms) so that the equilibrium distribution of D_2O, i.e., the deuterium density, could be determined. Signal in the deuterium reference image came primarily from the D_2O injected before the day of the MR experiment, which was assumed to have reached its equilibrium distribution.

Subsequently, a set of deuterium images was acquired rapidly before and after intravenous injection of D_2O. A 0.5-ml bolus of D_2O was injected into the external jugular vein over 2 s. The deuterium signal was detected using the 2.5-cm inner-diameter saddle coil. A slice thickness of 1.3 cm was necessary to obtain acceptable signal-to-noise ratio (SNR). A pulse angle of 45° was used with a short TR (TR = 320 ms) to maximize signal-to-noise ratio. SNR was further improved by optimizing detector bandwidth; because of the long T_2* (i.e., narrow linewidth) of the deuterium resonance in each image pixel, a long acquisition time (12 ms) and low amplitude readout gradients could be used. These adjustments resulted in T_2* and T_1 weighting of the image intensity, and this was taken into account in the data analysis (see below). In-plane spatial resolution was 2 mm with image acquisition time of 20 s. Deuterium images were obtained beginning before injection and ending 10 min after injection. This procedure was repeated three times - i.e., D_2O was injected three times so that three separate measurements of the kinetics of D_2O uptake were made. The D_2O injections were separated by 30 min to allow the animal time to recover from the fluid volume.

After deuterium measurements, the proton coil was reconnected and the preamplifier was tuned for protons. Subsequently T_1-weighted FLASH images with 500 ms time resolution were obtained before (20 images) and for 15 min after intravenous injection of 0.2 mMoles/kg Gd-DTPA-dimeglumine (Berlex Laboratories, Wayne, NJ) (~0.2 ml bolus). A single contrast agent injection was performed. To minimize T_2* effects, the time between excitation and detection was minimized. The RF sinc pulse duration was 3.5 ms (two cycles), phase encode time was 1 ms, gradient rise time was 0.3 ms, the total time between the end of the excitation pulse and the center of the gradient echo ("TE") was 4.5 ms, and the acquisition time (i.e., duration of the readout gradient) was 2 ms. Image resolution was 1.5 × 0.75 mm in a 1.3-cm slice. A large slice thickness was used so that the slices in which Gd-DTPA-dimeglumine and D_2O uptake were measured were identical.

Measurements of contrast agent concentration assumed (see below) that the image intensity was weighted only by T_1 effects and not by T_2* effects. To verify that T_2* effects were negligible under these experimental conditions, we obtained water proton spectra with 500 ms time resolution and 2 Hz frequency resolution before and after bolus IV injection of contrast using a small (1-cm diametr) surface coil placed directly over the tumor. Under control conditions, the linewidth of the water signal was 60 Hz with signal-to-noise ratio of 1000:1. The width of the water resonance changed by less than 2 Hz during passage of the contrast bolus. This suggested that changes in T_2* due to the contrast agent would not significantly affect the intensity of the FLASH images with echo times of less than 5 ms.

Theory: Perfusion Rate and Extraction Fraction

The extraction fraction (E) is the fraction of contrast agent molecules that exchange across capillary walls during a single passage through the capillary bed (i.e., during the mean transit time). The extraction fraction depends on capillary permeability as well as capillary surface area and mean transit time of blood through capillaries. Although almost all (~99.9%) of the capillary surface area in normal tissue is covered by the plasma membranes of endothelial cells, the remaining fraction of the surface area allows effective solute transport (27). Even more surface area is generally available in tumors. For Gd-DTPA-dimeglumine and similar small molecules, E is approximately 0.45 in most tissue except for brain where $E = 0$. "E" can be expressed as a function of the perfusion rate (F, in milliliters per hour 100 g):

$$E \equiv 1 - \exp(PS/F) \qquad [1]$$

where P the "permeability" of the vascular wall to the contrast agent and S is the surface area of vasculature per 100 g of tissue.

The change in the concentration of contrast agent in the extravascular compartment after bolus injection as a function of time, $C_T(t)$, has been modeled by a number of investigators (e.g., 10, 11, 20, 21, 33–37). For the purposes of the present study, the analysis can be simplified considerably. During the first pass of contrast after injection of an intravenous bolus, the transport of contrast from tissue to blood is negligible compared with the transport from blood to tissue so that the change in the number of Gd-DTPA molecules in the extravascular space in each image voxel (Q_T) can be approximated as:

$$\frac{dQ_T(t)}{dt} = F*E*C_B(t) \qquad [2]$$

where $C_B(t)$ = capillary blood concentration as a function of time.

Here we refer to the *number* of molecules rather than *concentration* so that there is no need to define the volume in which the contrast agent is distributed. The volume of distribution does not affect the number of contrast agent molecules that enter the extravascular space at short times after injection when the transport of contrast agent is primarily unidirectional, from blood to tissue. Integrating over the first pass of the bolus:

$$\Delta Q_T(t_f) = F*E*\int_{t_i}^{t_f} C_B(t) \cdot dt \qquad [3]$$

where t_i is a time just before the bolus enters the capillary bed and t_f is a time during the first passage of the bolus through the capillary bed but before the arrival of the second pass. $\Delta Q_T(t_f)$ is the amount of contrast agent (number of molecules per pixel) that enters the extravascular space during the interval t_i to t_f. We assume that the concentration of contrast agent in capillary blood as a function of time, $C_B(t)$, is the same for all tissues; this is accurate, as long as differences in the arrival time of the bolus in each tissue are properly accounted for.

Contrast agent uptake during the first pass, $\Delta Q_T(t_f)$, is proportional to "$F \times E$" and can be used to determine the relative value of "$F \times E$" in different regions of interest (ROIs) (e.g., muscle versus tumor center). However, $\Delta Q_T(t_f)$ is most accurately determined *after* the contrast bolus has passed through the capillary beds. At the peak of the bolus, the large contrast agent concentration in capillary blood (~50 m*M*) may complicate analysis of the data. In addition, spin systems may take some time to respond to changes in T_1 caused by changing concentrations of the contrast agent in the tissue. This response time is similar to the time required for longitudinal magnetization to reach a steady state at the beginning of the dynamic imaging sequence—approximately 1 s under the current experimental conditions. To minimize these problems ΔQ_T was measured at a time t_f after the bulk of the first pass of contrast agent, but before the second pass had arrived. This time was determined from the capillary input function. (We define the capillary input function as the concentration of contrast agent in capillary blood as a function of time, $C_B(t)$; see Eq. [3].) An estimate of the capillary input function is calculated from the tissue contrast agent concentration curves.

Figure 1a shows a typical plot of Gd concentration versus time in muscle after bolus intravenous injection. The increase in signal due to the contrast agent is primarily due to contrast agent molecules that are extracted from the vasculature into tissue. For purposes of qualitative analysis, we ignore the contribution from the contrast agent that remains in the blood, which is smaller than that of contrast agent molecules in the extravascular space. (This approximation is supported by the fact that intravascular agents provide poor T_1 contrast (e.g., 34) compared with contrast agents that are extracted.) Therefore, the derivative of the plot of the measured contrast agent concentration as a function of time (Fig. 1b) is approximately proportional to $C_B(t)$ (i.e., the capillary input function; see Eq. [3]). The gamma variate fit (35, 36) to the input function is also shown. The first pass of contrast agent through tissue is evident between 45 and 55 s. The second and subsequent passes also appear beginning at approximately 65 s. The gamma variate fit allows determination of the point at which 90% of the first pass of the bolus is complete (t_f). Figure 1b shows that at this point there is very little recirculation.

If the capillary input function is equal everywhere in the slice imaged by MR, then just after the first pass of the contrast bolus (t_f) Eq. [3] simplifies to:

$$\Delta Q_T(t_f) \alpha\ F \cdot E \qquad [4]$$

Classical multiple-indicator methods (37) allow measurement of both F and $F \times E$ individually and, thus, greatly facilitate interpretation of dynamic contrast agent data. Since the extraction fraction of D_2O, E_{D_2O}, is ~1.0 at flow rates which occur in tumor and skeletal muscle *in vivo*, time resolved measurements of D_2O uptake give accurate relative and/or absolute measurements of tissue perfusion rate, i.e., $F*E_{D_2O} = F$ (11–15, 17, 38). Measurements of Gd-DTPA-dimeglumine uptake yield "$F \times E_{Gd}$" to within a proportionality constant, where "E_{Gd}" is the extraction fraction. Comparison of D_2O and Gd-DTPA-dimeglumine uptake allows calculation of both F and E_{Gd}. Relative $F \times E_{Gd}$ is divided by relative F (determined from D_2O uptake) to determine relative E_{Gd}.

Analysis of Deuterium Uptake Data

Data analysis was performed using IDL (Boulder, CO) on a Sun Sparc 10 (Mountain View, CA) D_2O uptake data were analyzed following the method of Mattiello and Evelhoch (16) to measure the relative tissue perfusion rate. Deuterium density images obtained after 3 days of intraperitoneal injections of D_2O were isotense except in bone, demonstrating that D_2O was uniformly distributed at equilibrium and that the RF field of the coil was relatively homogeneous. This is expected since the wet weight of tissue is relatively uniform. This means that spatial variations in pixel intensity in control images (i.e., in "fast" images obtained immediately before intravenous D_2O injection when D_2O is approximately in an equilibrium distribution) reflect differences in T_2* and T_1. Small variations in RF field strength may also be a factor, since these fast T_1 weighted images are more sensitive to pulse angle than the deuterium density images obtained with a 45° pulse angle. Since the true concentration of D_2O during the control period was known to be uniform, intensity measured in each pixel of the "fast" images was normalized to the control image intensity and changes in the normalized intensity were taken to be proportional to changes in D_2O concentration:

$$\Delta D_2O \sim \Delta \text{ Normalized Pixel Intensity}(t)$$

$$= \frac{(\text{Intensity}(t) - \text{Control Intensity})}{\text{Control Intensity}} \qquad [5]$$

Based on normalized D_2O images, regions of interest were selected in tumor and surrounding muscle (same ROIs used for Gd-DTPA-dimeglumine uptake analysis). For each of these ROIs, the average deuterium concentra-

tion as a function of time was calculated. At early time points, D_2O uptake in tissue is proportional to tumor perfusion rate assuming that the capillary input function is the same in all tissues (39). Differences in the "arrival time" of the D_2O bolus in capillaries are of limited importance for data with time resolution of 20 s and these effects can be accounted for during data analysis. (At later time points (39), tracer distribution is more representative of the equilibrium distribution, i.e., in the case of D_2O, of tissue water content.) The relative perfusion rates for the ROIs were estimated by integrating the change in D_2O concentration as a function of time from 20 s after D_2O injection to 120 s after D_2O injection (to minimize sensitivity to the shape of the input function) (16).

Analysis of Gd-DTPA Uptake Data

The T_1-weighted images obtained before and after Gd-DTPA-dimeglumine injection and a fully relaxed image were used to estimate Gadolinium concentration. Assuming that there were no significant T_2* effects, these measurements are accurate at contrast agent concentrations below several m*M* (40). Gadolinium concentration was estimated (41, 42) from:

$$C(t) = \frac{1}{TR \cdot R1} \cdot \left[\ln\left[\frac{S_o \cdot \sin \vartheta - S_b}{S_o \cdot \sin \vartheta - S_b \cdot \cos \vartheta} \right] - \ln\left[\frac{S_o \cdot \sin \vartheta - S_a(t)}{S_o \cdot \sin \vartheta - S_a(t) \cdot \cos \vartheta} \right] \right] \quad [6]$$

where $C(t) \equiv$ the contrast agent concentration as a function of time, $TR \equiv$ repetition time (15 ms), R1 ≡ longitudinal relaxivity of Gadolinium-DTPA-dimeglumine (~4.4 mM^{-1} s^{-1} at 4.7 T; extrapolated 43–49), $S_o \equiv$ thermal equilibrium signal intensity measured using a 90° pulse, $S_a(t) \equiv$ the MR signal intensity as a function of time after contrast agent injection, $S_b \equiv$ the MR signal intensity before contrast agent injection, ~45° ≡ ϑ (pulse angle). Note that the term "concentration" in this equation refers to the contrast agent concentration averaged over the entire image voxel (i.e., the number of contrast agent molecules, Q, in each voxel is divided by the volume of the aqueous space in the voxel). This is a reasonable approximation since at concentrations of Gadolinium below several millimolar the entire extravascular space behaves as a single well mixed compartment. All water molecules have equal access to Gadolinium due to rapid exchange of water across cell membranes. The Gadolinium concentration in the blood need not be considered, since it is negligible at time "t_f". With these approximations, concentrations of Gd-DTPA-dimeglumine determined from Eq. [6] together with the D_2O concentration determined from Eq. [5] were used to solve Eq. [4] for relative "$F \times E_{Gd}$" and F.

RESULTS

Reproducibility

Blood pressure was 120 ± 20 mmHg during 4–5 h of ketamine and rompun anesthesia (in all tumors studied). In this same tumor model, hemoglobin oxygen saturation did not fall below 95% and temperature was maintained between 36°C and 38°C over 4 h (31, 32). Repeated measurements in the same tumor model showed no significant changes in contrast agent uptake during the first pass after bolus intravenous injection over a 4 hour period (4 - 5 bolus injections of contrast agent over a 4-h period). The amount of contrast agent taken up by tumor and muscle tissue during the first pass varied by no more than 10% (i.e., the standard deviation for repeated measurements, n = 4, was 10%), and there was no significant decrease with time. For Gd-DTPA-dimeglumine injections, the "first pass" of the contrast agent bolus estimated from the derivative of the tissue contrast agent concentration curves in both tumor and muscle was clearly detected with some evidence of later passes (see Fig. 1). When contrast agent uptake during the first pass in tumor was divided by the muscle value (determined at t_f) to obtain relative "$F \times E$", the average standard deviation per experiment was no more than 15%. This suggests that perfusion rate was stable over the course of the experiment.

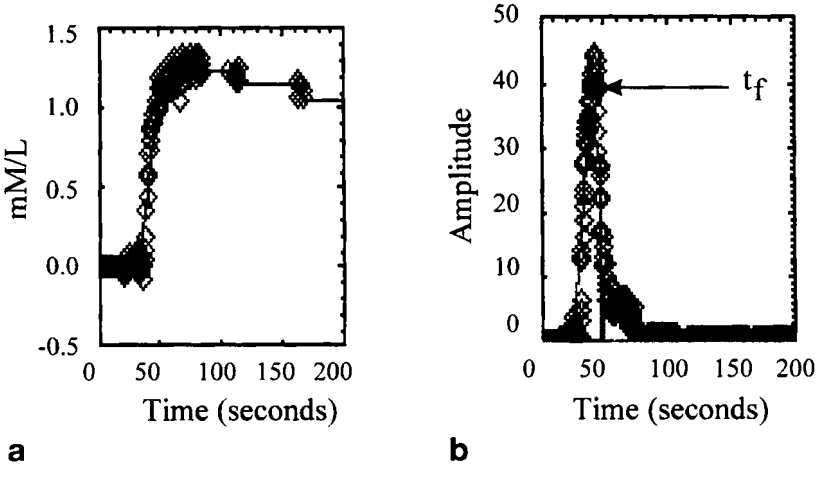

FIG. 1. (a) Typical plot of concentration versus time for Gadolinium-DTPA-dimeglumine in muscle after bolus intravenous injection. (b) The plot is proportional to the concentration of contrast in capillary blood (i.e., the capillary input function; solid line). A gamma variate fit to the input function is also shown (dashed line).

Histology and Evans Blue

Histological slices were taken from the same slices as the MRI data. Histology indicated little necrosis in the tumor regions. Evans Blue uptake (an indicator of vascular permeability) was evaluated in the slice that was imaged by MR. Evans Blue was highly extracted in tumor compared with muscle tissue and extraction was highest at the interface between tumor and mus-

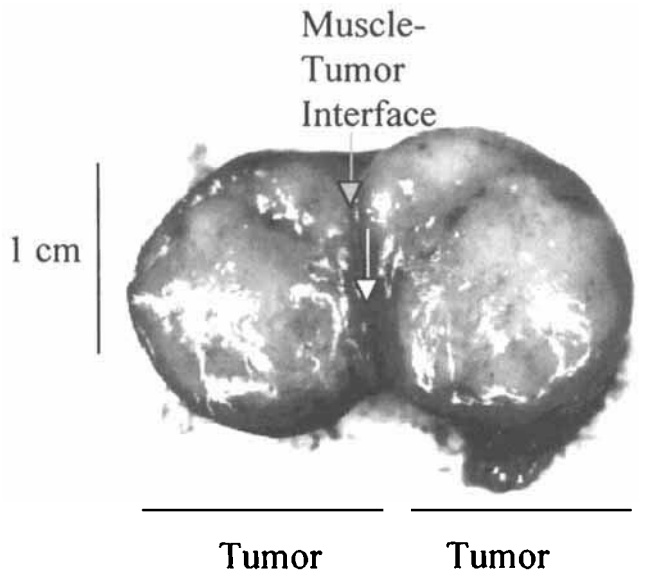

FIG. 2. An excised mammary adenocarcinoma after Evans Blue injection. The white arrows close to the muscle-tumor interface indicate areas of highest Evans Blue uptake.

cle. Figure 2 shows an excised mammary adenocarcinoma after Evans Blue injection. The tumor in Fig. 2 was cut open along the same slice as the MR slice, i.e., cuts were made in the tumor starting distal to the body moving proximal. The arrows close to the muscle-tumor interface indicate areas of highest Evans Blue uptake. It should be noted that very bright areas (i.e., white) in Fig. 2 are due to glare and do not represent lack of Evans Blue uptake.

Relative Perfusion Rate and Extraction Fraction Results

The signal-to-noise ratio for measurement of D_2O uptake in a typical ROI (5 × 2.5 mm) was ~10:1. Figure 3a shows an example of a post-D_2O injection image. The figure is a summation of images taken from 20 to 120 s after D_2O injection. Figs. 3b and 3c illustrate changes in MR intensity before, during, and after D_2O injection. Figure 3b shows a plot of Deuterium signal intensity versus time in a tumor ROI. The time period over which D_2O concentration was integrated to obtain relative perfusion rate is shown in black. Data shown in Figs. 3b and 3c were taken with no intraperitoneal D_2O injections previous to the day of the experiment.

SNR for measurement of Gd-DTPA uptake in a typical ROI was ~70:1. Figure 4 shows changes in MR intensity before, during, and after Gd-DTPA-dimeglumine injection. A typical plot of contrast agent concentration versus time is shown in Fig. 1a.

Figure 5 shows a summary of data from all of the tumors studied (n = 9). Average perfusion rate and extraction fraction are given for regions of interest defined (based on high resolution images) in the tumor center, the tumor rim, the tumor-muscle interface, and in muscle. (In Fig. 5a: "**" means that the value in a given ROI is significantly different from the value in muscle, $P < 0.005$ by paired t test and "*" indicates $P < 0.01$ by paired t test. Values are given relative to muscle. The error bars represent the standard errors of the pooled results). The perfusion rate, F, determined from D_2O uptake was significantly higher in the tumor center and tumor rim than in muscle.

Figure 5b shows extraction fraction relative to muscle for Gd-DTPA-dimeglumine. The extraction fraction was highest at the muscle-tumor interface in each of nine experiments—an average of *two times greater than in muscle ($P < 0.005$ by paired t test).* (The muscle-tumor interface is the region in which the tumor joins the muscle (see Figs. 2 and 6.)) The extraction fraction is also higher at the tumor center than in muscle ($P < 0.01$ by paired t test). Figure 6 shows results from a representative experiment. Figure 6a is an image in which intensity is proportional to relative perfusion rate superimposed on a reference image of the tumor-bearing hind limb. Figure 6b shows an image in which intensity is proportional to Gd-DTPA-dimeglumine extraction fraction. The high extraction fraction at the interface between tumor and muscle is evident. This corresponds to the distribution of tissue uptake of Evans Blue (see Fig. 2).

DISCUSSION

These results demonstrate that fully extractable (e.g., D_2O) and less extractable (e.g., Gd-DTPA-dimeglumine) MR detectable tracers can be used in concert to provide tissue contrast agent extraction fraction and perfusion information. The relative extraction fraction was higher in tumor than in muscle and highest at the interface between tumor and muscle. Assuming that muscle has an extraction fraction of 0.45, the extraction fraction at the muscle-tumor interface was close to 1.0, i.e., Gd-DTPA-dimeglumine in this region is approximately 100% extracted. Evans Blue results demonstrate that capillary permeability is high in the tumor and highest at the tumor muscle interface. Thus a high extraction fraction of Gd-DTPA-dimeglumine correlates with high capillary permeability in this model system. The high rate of perfusion in the tumor suggests that the tumor is metabolically active and that tumor vascular density is high. Rapid perfusion combined with high capillary permeability suggests rapid tumor growth and angiogenesis (50). This type of information could be used clinically to identify areas of angiogenic activity and thus differentiate malignant and invasive cancers from more benign tumors. It is likely that fully extractable MR contrast agents which can be substituted for D_2O can be used to increase signal-to-noise ratio and spatial resolution of the measurement.

Error in the measurement of extraction fraction was on the order of 20%. D_2O measurements were the main source of errors. This indicates that changes in extraction fraction of 0.1 can be detected since normal tissue Gd-DTPA-dimeglumine extraction fraction is ~0.45 (10). Once relative extraction fraction and flow estimates are made, estimates of absolute perfusion rate and extraction fraction can be obtained if flow and extraction fraction have been measured (or estimated) in a reference tissue, e.g., rat skeletal muscle.

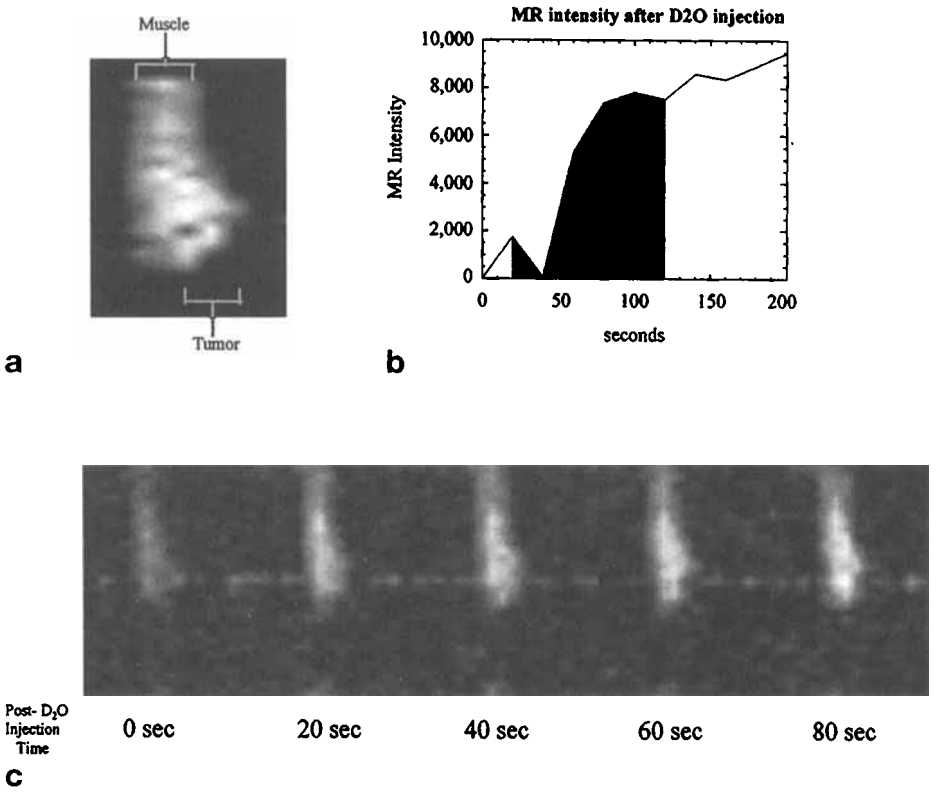

FIG. 3. (a) Image shows an example of a post-D_2O injection image (image shown is a summation of images taken from 20 to 120 s after D_2O injection). (b) A plot of changes in MR intensity before, during, and after D_2O injection. The shading shows the time period over which D_2O signal is integrated to obtain relative perfusion rate. (c) Images of changes in MR intensity before, during, and after D_2O injection.

The measurements of capillary permeability and contrast agent extraction fraction presented here are based on a number of assumptions which are discussed below:

1. In healthy tissue, Gd-DTPA-dimeglumine is concentrated in the extracellular space. However, the entire extravascular compartment is treated as a single well-mixed compartment, and the concentration of contrast agent is given in units of "moles per liter of tissue water," since to a good approximation (51), water molecules in all extravascular compartments have access to contrast agent molecules on a time scale that is fast compared with T_1. Thus, under most conditions, the longitudinal relaxation rate of all water molecules in the extravascular space is equally influenced by Gd (52), as long as the Gd concentration is less than several millimolar.
2. A linear dependence of relaxivity on contrast agent concentration is assumed. This relationship is reliable at Gd concentrations less than several millimolar (e.g., 40, 52) and when losses due to T_2* relaxation during the excitation, phase encoding, and readout periods are minimized or accounted for.
3. The pulse rotation angle is assumed to be spatially homogeneous. Since very thick (1.3 cm) slices were used, the volumes of the edge regions where pulse angle is inhomogeneous were negligible compared with the volume in which pulse angle is constant.
4. Complications caused by high blood concentrations of Gd-DTPA-dimeglumine and slow response of the spin system to changes in T_1 are assumed to be minimized by measuring the tissue concentration of Gd after most of the first pass of the contrast agent bolus is completed.
5. The relaxivity of Gd is assumed to be the same in all of the environments that are imaged. Support for this assumption comes from studies that showed that the relaxivity of Gd is the same in saline, plasma, cartilage, and trypsinized cartilage (52). This is primarily because Gd is tightly bound by DTPA and is unlikely to interact strongly with other molecules which might change its correlation time or electronic relaxation time.
6. Tumors and surrounding tissue were assumed to be hemodynamically stable so that blood flow patterns were the same during Gd and D_2O uptake. The present results as well as previous results obtained in this laboratory (31, 32) suggest that this is a valid assumption.
7. The low resolution of the D_2O images resulted in partial volume effects. It was assumed that normalization of changes in MR signal intensity following D_2O injection,

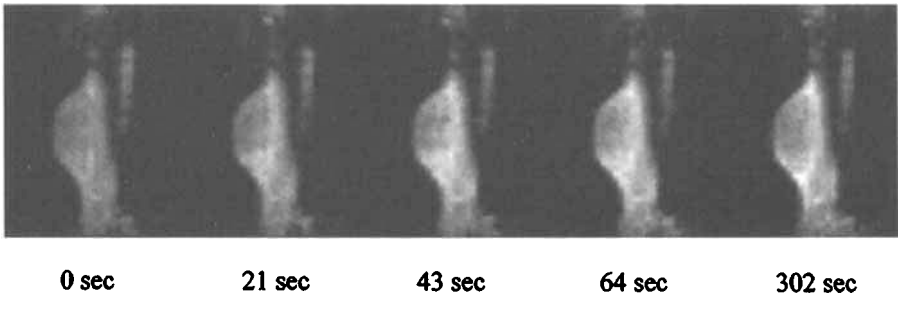

FIG. 4. Images of changes in MR intensity before, during, and after Gd-DTPA-dimeglumine injection.

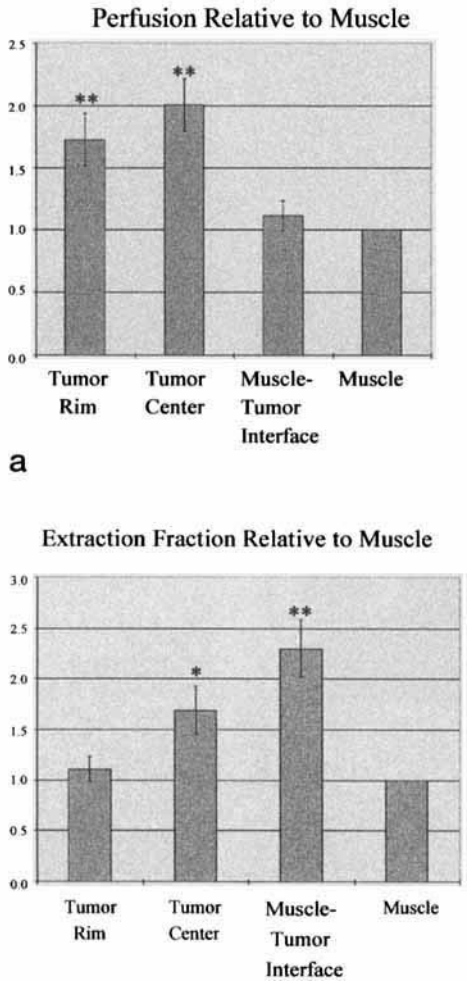

FIG. 5. (a) Relative (to muscle) tissue perfusion rate. ** indicates that perfusion rate in the indicated region was significantly different from perfusion rate in muscle; $P < 0.005$ by paired t test. * indicates $P < 0.01$ by paired t test. (b) Relative (to muscle) Gd-DTPA dimeglumine extraction fraction. ** indicates that extraction fraction in the indicated region was significantly different from extraction fraction in muscle; $P < 0.005$ by paired t test. * indicates $P < 0.01$ by paired t test.

based on control image intensity, gave an accurate measure of tissue uptake of D_2O. In pixels that were only half-filled with tissue, i.e., in pixels at the edge of tumor and muscle or in pixels containing bone, normalization corrects for the reduction in signal intensity caused by partial volume effects.

8. Hemodynamic properties were assumed to be homogeneous within each image voxel.
9. Observation of a relatively high extraction fraction in tumors could be due to a long bolus mean transit time (MTT) through the capillaries, rather than to high capillary permeability. Slower MTTs would allow more fluid exchange and thus larger extraction fraction. The higher perfusion rate in tumors suggests that MTT in tumors is *not* slower than in muscle but this is not unequivocal proof since perfusion rate depends on *both* MTT and vascular density or volume.

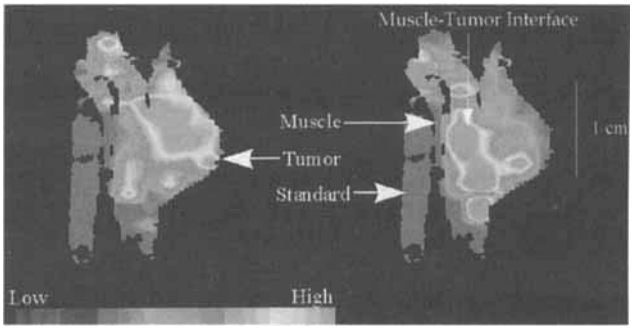

FIG. 6. (a) Image intensity is proportional to relative perfusion rate superimposed on a reference image of the tumor-bearing hind limb. The brighter the intensity the greater the relative perfusion rate. (b) Image intensity is proportional to relative extraction fraction superimposed on a reference image of the tumor-bearing hind limb. The brighter the intensity the greater the extraction fraction.

The double indicator technique demonstrated here may improve understanding of the dynamics of tissue uptake of Gd-DTPA derivatives in highly metastatic and less aggressive tumors. *In addition,* Gd-DTPA derivatives combined with D_2O could be used clinically to characterize tumors. However, the technique would probably be useful only for studies of superficial human tumors, due to the limited spatial resolution of deuterium imaging. Because of the low SNR of D_2O images, the D_2O perfusion estimates may mask tumor pathophysiological heterogeneity. This problem could be avoided if MR contrast agents which, like D_2O, are 100% extracted, are available. The methodology described in this paper indicates that fully extractable contrast agents could be used in combination with partially extractable low molecular weight contrast agents—perhaps with extraction fractions even lower than that of Gd-DTPA dimeglumine—to determine perfusion rate and vascular permeability with high spatial resolution. Therefore, development of a highly extractable Gd chelate is highly desirable. Dynamic imaging of myocardial uptake of Gadodiamide (Nycomed, Princeton, NJ) suggests that this contrast agent may be highly extracted (53). Work in this laboratory performed in collaboration with Mukherjee *et al.* demonstrates that a Gadolinium iminodiacetic acid complex may be fully extractable (54). These compounds would probably provide spatial resolution for perfusion rate and extraction fraction measurements on the order of 1 mm in-plane in a 2-mm thick slice.

Information obtained from double indicator studies may lead to improved procedures for detection and analysis of uptake of Gd-DTPA derivatives so that tumor grade can be measured using Gd-DTPA alone. For example, it is possible that simultaneous measurements of changes in T_1 and T_2* during contrast agent uptake may allow estimation of perfusion rate and extraction fraction (34, 55). Such a method would be developed and evaluated using the double indicator method as a gold standard.

In addition to studies of tumor vasculature, there are a variety of applications where measurement of capillary permeability combined with perfusion measurement based on uptake of low molecular weight contrast agents

would be beneficial. For example, increased vascular permeability could be measured in damaged myocardium (52, 56–59), in lungs due to oxygen-induced pulmonary injury (60), and in muscle due to electrical injury.

CONCLUSIONS

Low molecular weight Gd-DTPA derivatives are in widespread clinical use and extraction fraction is a critical determinant of image contrast at early times following bolus injection. However, the extraction fractions of these molecules have not previously been imaged *in vivo*. A number of other investigators have developed models for the kinetics of contrast agent uptake which can provide information concerning capillary permeability and perfusion rate (61–63). The present approach may be more labor intensive than these analytical methods because it requires the use of two different tracers. However, the dual indicator method has the potential to provide quantitative measurements of low molecular weight contrast agent extraction fractions under a wide range of conditions. The present results illustrate that *in vivo* images of the relative extraction fraction of a Gd-DTPA derivative can be produced under the condition that the rate of contrast agent extraction across capillary walls and the rate of contrast agent delivery via blood flow are similar. The primary limitation of the technique is signal-to-noise ratio and/or spatial resolution, but this problem could be solved by using highly diffusible MR contrast agents as a substitute for D_2O.

REFERENCES

1. N. Weidner, J. Folkman, F. Pozza, P. Bevilacqua, E. N. Allred, D. H. Moore, S. Meli, G. Gasparini, Tumor angiogenesis: a new significant and independent prognostic indicator in early-stage breast carcinoma. *J. Natl. Cancer Inst.* **84,** 1875–1851 (1992).
2. A. J. Guidi, L. Fischer, J. R. Harris, S. J. Schnitt, Microvessel density and distribution in ductal carcinoma in situ of the breast. *J. Natl. Cancer Inst.* **86,** 614–619 (1994).
3. C. Frouge, J-M Guinebretier, G. Contesso, R. Di Paola, M. Blery, Correlation between contrast enhancement in dynamic magnetic resonance imaging of the breast and tumor angiogenesis. *Invest. Radiol.* **29,** 1043–1049 (1994).
4. H. F. Dvorak, J. A. Nagy, B. Berse, L. F. Brown, K-T Yeo, T-K Yeo, A. M. Dvorak, L. van de Water, T. M. Sioussat, D. R. Senger, Vascular permeability factor, fibrin, the pathogenesis of tumor stroma formation. *Ann. N.Y. Acad. Sci.* **667,** 101–111 (1992).
5. L. F. Brown, A. M. Dvorak, H. F. Dvorak, Leaky Vessels, Fibrin deposition and fibrosis: a sequence of events common to solid tumors and to many other types of disease. *Am. Rev. Respir. Dis.* **140,** 1104–1107 (1989).
6. D. R. Senger, L. Van De Water, L. F. Brown, J. A. Nagy, K-T Yeo, T-K Yeo, B. Berse, R. W. Jackman, A. M. Dvorak, H. F. Dvorak, Vascular permeability factor (VPF, VEGF) in tumor biology. *Cancer Metastasis Rev.* **12,** 303–324 (1993).
7. L. E. Gerlowski, R. K. Jain, Microvascular permeability of normal and neoplastic tissues. *Microvasc. Res.* **31,** 288–305 (1986).
8. H. J. Weinmann, R. C. Brasch, W. R. Press, G. E. Wesbey, Characteristics of gadolinium-DTPA complex: a potential NMR contrast agent. *Am. J. Roentol.* **142,** 619 (1984).
9. F. S. Prato, G. Wisenberg, T. P. Marshall, P. Uksik, P. Zabel, Comparison of the biodistribution of gadolinium-153 DTPA and technicium-99 M DTPA in rats. *J. Nucl. Med.* **29,** 1683 (1988).
10. L. D. Diesbourg, F. S. Prato, G. Wisenberg, D. J. Drost, T. P. Marshall, S. E. Carroll, B. O'Neill, Quantification of myocardial blood flow and extracellular volumes using a bolus injection of gd-dtpa: kinetic modeling in canine ischemic disease. *Magn. Reson. Med.* **23,** 239–253 (1992).
11. S-G Kim, J. J. H. Ackerman, Quantification of regional blood flow by monitoring of exogenous tracer via nuclear magnetic resonance spectroscopy. *Magn. Reson. Med.* **14,** 266–282 (1990).
12. J. J. Neil, S-K Song, J. J. H. Ackerman, Concurrent quantification of tissue metabolism and blood flow via $^{2}H/^{31}P$ NMR *in vivo*. II. Validation of the deuterium NMR washout method for measuring organ perfusion. *Magn. Reson. Med.* **25,** 56–66 (1992).
13. S-K Song, R. S. Hotchkiss, I. E. Karl, J. J. H. Ackerman, Concurrent quantification of tissue metabolism and blood flow via $^{2}H/^{31}P$ NMR *in vivo*. III. Alterations of muscle blood flow and metabolism during sepsis. *Magn. Reson. Med.* **25,** 67–77 (1992).
14. S-K Song, R. S. Hotchkiss, J. J. H. Ackerman, Concurrent quantification of tissue metabolism and blood flow via $^{22}H/^{31}P$ NMR *in vivo*. I. Assessment of absolute metabolite quantification. *Magn. Reson. Med.* **25,** 45–55 (1992).
15. S-G Kim, J. J. H. Ackerman, Quantitative determination of tumor blood flow and perfusion via deuterium nuclear magnetic resonance spectroscopy in mice. *Cancer Res.* **48,** 3449–3453 (1988).
16. J. Mattiello, J. L. Evelhoc, Relative volume-average murine tumor blood flow measurement via deuterium nuclear magnetic resonance spectroscopy. *Magn. Reson. Med.* **18,** 320–334 (1991).
17. J. B. Larcombe McDouall, J. L. Evelhoch, Deuterium nuclear magnetic resonance imaging of tracer distribution in d_2o clearance measurements of tumor blood flow in mice. *Cancer Res.* **50,** 363–369 (1990).
18. M. R. Tripp, M. W. Meyer, S. Einzig, J. J. Leonard, C. R. Swayzee, J. Fox, Simultaneous regional myocardial blood flows by tritiated water and microspheres. *Am. J. Physiol.* **232,** H173–H190 (1977).
19. F. M. Cohen, R. Kuwatsuru, S. Shames, M. Neuder, J. S. Mann, V. Vexler, W. Rosenau, R. C. Brasch, Contrast-enhanced magnetic resonance imaging estimation of altered capillary permeability in experimental mammary carcinomas after x-irradiation. *Invest. Radiol.* **29,** 970–977 (1994).
20. R. Jain, L. Gerlowshi, Extravascular transport in normal and tumor tissues. *Crit. Rev. Onco. Hematol.* **5,** 115–170 (1984).
21. R. Jain, Transport of molecules across tumor vasculature. *Cancer Metastasis Rev.* **6,** 559–593 (1987).
22. R. Jain, Vascular and interstitial carriers to delivery of therapeutic agents in tumors. *Cancer Metastasis Rev.* **9,** 253–266 (1990).
23. L. Baster, R. Jain, Transport of fluid and macromolecules in tumors. III. Role of binding and metabolism. *Microvasc. Res.* **41,** 5–23 (1991).
24. S. Seymour, Passive tumor targeting of soluble macromolecules and drug conjugate. *Crit. Rev. Ther. Drug Carrier Syst.* **9,** 135–187 (1992).
25. K. P. Aicher, J. W. Dupon, D. L. White, S. L. Aukerman, M. E. Moseley, R. Juster, J. Rosenau, J. L. Winkelhate, R. C. Brasch, Contrast-enhanced magnetic resonance imaging of tumor-bearing mice treated with human recombinant tumor necrosis factor alpha. *Cancer Res.* **50,** 7376–7381 (1990).
26. H. Maeda, L. Seymour, Y. Miyamoto, Conjugates of anticancer agents and polymers: advantages of macromolecular therapeutics in vivo. *Bioconjug. Chem.* **3,** 351–362 (1992).
27. C. Crone, D. G. Levitt, *in* "Handbook of Physiology", (E. Renkin, C. C. Michel, S. R. Geiger, Eds.), Vol IV, Print I, American Physiology Society, Bethesda, MD, 1984.
28. M. Inge, C. Bell, J. J. Freeman, A. Barna, Biochemical and morphologic properties of a new lactating mammary tumor line in the rat. *Cancer Res.* **25,** 286–299 (1965).
29. C. E. Hayes, W. A. Edelstein, J. F. Schenck, O. M. Mueller, M. Eash, An Efficient, Highly homogeneous radiofrequency coil for whole-body nmr imaging at 1.5 T. *J. Magn. Reson.* **63,** 622–628 (1985).
30. J. Tropp, The theory of the bird-cage resonator. *J. Magn. Reson.* **82,** 51–62 (1989).
31. G. S. Karczmar, J. N. River, K. L. Liu, Detection of tumor perfusion using radio frequency gradients. *J. Magn. Reson. Imaging* **1,** 203 (1991).
32. G. S. Karczmar, J. N. River, K. L. Liu, Non-invasive measurement of tumor perfusion by magnetic resonance, *in* "Proc., AUR, 39th Annual Meeting, Orlando, 1991," p. 87.
33. D. A. Kovar, G. S. Karczmar, Analysis of dynamic mr contrast uptake measurements: theory and application, *in* "Proc., ISMRM, 4th Scientific Meeting, New York, 1996," p. 1597.
34. D. M. Shames, R. Kuwatsuru, V. Vexler, A. Muhler, R. C. Brasch, Measurement of capillary permeability to macromolecules by dynamic magnetic resonance imaging: a quantitative noninvasive tech-

nique. *Magn. Reson. Med.* **29,** 616–622 (1993).
35. M. M. Bahn, A single-step method for estimation of local cerebral blood volume from susceptibility contrast mri images. *Magn. Reson. Med.* **33,** 309–317 (1995).
36. H. K. Thompson, C. F. Starmer, R. E. Whalen, H. D. McIntosh, Indicator transit time considered as a gamma variate. *Circ. Res.* **14,** 502–515 (1964).
37. N. A. Lassen, W. Perl, "Tracer Kinetic Methods in Medical Physiology," pp. 1–189, Raven Press, New York, 1979.
38. B. D. Ross, S. L. Mitchell, H. Merkle, M. Garwood, *In vivo* ^{31}P and ^{1}H NMR studies of rat brain tumor ph and blood flow during acute hyperglycemia: differential effects between subcutaneous and intracerbral locations. Magn. Reson. Med. 12, 219–234 (1989).
39. L. A. Sappirstein, Regional blood flow by fractional distribution of indicators. *Am. J. Physiol.* **193,** 161–168 (1958).
40. P. M. Parizel, B. A. A.M. van Hasselt, L. van den Hauwe, J. W. M. Van Goethem, A. M. A. DeSchepper. Effect of field strength on gadolinium enhancement in MR imaging. *Eur. Radiol.* **4,** 557–560 (1994).
41. P. Bendel, T_2-weighted contrasts in rapid low flip-angle imaging. *Magn. Reson. Med.* **5,** 366–370 (1987).
42. K. Hittmair, G. Gomiscek, K. Langenberger, M. Recht, H. Imhof, J. Kramer, Method for quantitative assessment of contrast agent uptake in dynamic contrast-enhanced MRI. *Magn. Reson. Med.* **31,** 567–571 (1994).
43. R. B. Lauffer, *in* "Clinical Magnetic Resonance Imaging" (R. R. Edelmann, J. R. Hesselink, Eds.), p. 225, Saunders, Philadelphia, 1990.
44. E. C. Unger, K. Ugurbil, R. Latchan, Contrast agents for cerebral perfusion imaging. *J. Magn. Reson. Imaging* **4,** 235–242 (1994).
45. S. D. Kennedy, L. S. Szczepaniak, S. L. Gibson, R. Hilf, T. H. Foster, R. G. Bryant, Quantitative MRI of Gd-DTPA uptake in tumors: response to photodynamic therapy. *Magn. Reson. Med.* **31,** 292–301 (1994)
46. S. Schaefer, R. A. Lange, P. V. Kulkarni, J. Katz, R. W. Parkey, J. T. Willerson, R. M. Peshock, In vivo NMR imaging of myocardial perfusion using the paramagnetic contrast agent manganesse gluconate. *J. Am. College of Cardiol.* **14,** 472–80 (1989).
47. K. M. Donahue, D. Burstein, W. J. Manning, M. L. Gray, Studies of Gd-DTPA relaxivity and proton exchange rates in tissue. *Magn. Reson. Med.* **32,** 66–76 (1994).
48. H-J Weinmann, M. Laniado, W. Mutzel, Pharmokinetics of Gd-DTPA/dimeglumine after intravenous injection into healthy volunteers. *Physiol. Chem. Physics Med. NMR* **16,** 167–173 (1984).
49. H-J Weinmann, R. C. Brasch, W-R Press, G. E. Wesbey, Characteristics of gadolinium-DTPA complex: a potential NMR contrast agent. *Am. J. Roentgenol.* **142,** 619–624 (1984).
50. H. F. Dvorak, M. Detmar, K. P. Claffey, J. A. Nagy, L. van de Water, D. R. Senger, Vascular permeability factor/vascular endothelial growth factor: an important mediator of angiogenesis in malignancy and inflammation. *Inter. Arch. Allergy Immunol.* **107,** 233–235 (1995).
51. K. M. Donahue, D. Burstein, W. J. Manning, M. C. Gray, Studies of Gd-DTPA relaxivity and proton exchange rates in tissue. *Magn. Reson. Med.* **32,** 66–76 (1994).
52. L. D. Diesbourg, F. S. Prato, G. Wisenberg, D. J. Drost, Marshall, S. E. Carroll, B. O'Neill, Quantification of myocardial blood flow and extracellular volumes using a bolus injection of Gd-DTPA: kinetic modeling in canine ischemic disease. *Magn. Reson. Med.* **23,** 239–253 (1992).
53. M. F. Wendland, M. Saeed, T. Masui, N. Derugin, M. E. Moseley, C. B. Higgins, Echo-planar MR imaging of normal and ischemic myocardium with gadodiamide injection. *Radiology* **186,** 535–542 (1993).
54. D. A. Kovar, J. Mukherjee, M. Z. Lewis, M. J. Lipton, G. S. Karczmar, Uptake kinetics of a *new* highly permeable gadolinium-chelate, *in* "Proc, RSNA Scientific Program, Chicago, 1996," p. 391.
55. V. Y. Kuperman, G. S. Karczmar, M. J. K. Blomley, M. Z. Lewis, L. M. Lubich, M. J. Lipton, Differentiating between T1 and T2* changes caused by gadopentetate dimeglumine in the kidney by using a double-echo dynamic MR imaging sequence. *J. Magn. Res. Imaging* **6,** 764–768 (1996).
56. I. K. Adzamli, M. Blau, M. A. Pfeffer, M. A. Davis, Phosphate-modified Gd-DTPA complexes III. The detection of myocardial infarction by MRI. *Magn. Reson. Med.* **29,** 505–511 (1993).
57. S. Schaefer, C. R. Malloy, J. Katz, R. W. Parkey, L. M. Buja, J. T. Willerson, R. M. Peshock, Gadolinium-DTPA-enhanced nuclear magnetic resonance imaging of reperfused myocardium: identification of the myocardial bed at risk. *J. Am. College Cardiol.* **12,** 1064–72 (1988).
58. N. Wilke, C. Simm, J. Zhang, J. Ellermann, X. Ya, H. Merkle, G. Path, H. Ludemann, R. J. Bache, K. Ugurbil, Contrast-enhanced first pass myocardial perfusion imaging: correlation between myocardial blood flow in dogs at rest and during hyperemia. *Magn. Reson. Med.* **29,** 485–497 (1993).
59. N. Wilke, K. Kroll, H. Merkle, Y. Wang, Y. Ishibaski, Y. Xu, J. Zhang, M. Jerosch-Herold, A. Muhler, A. Stillmann, J. B. Bassingthwaighte, R. Bache, K. Ugurbil, Regional myocardial blood volume and flow: first pass MR imaging with polylysine-Gd-DTPA. *J. Magn. Reson. Imaging* **5,** 227 (1995).
60. R. C. Brasch, Y. Berthezene, V. Vexler, W. Rosenau, O. Clement, A. Muhler, R. Kuwatsuru, D. M. Shames, Pulmonary oxygen toxicity: demonstration of abnormal capillary permeability using contrast-enhanced MRI. *Ped. Rad.* **23,** 495–500 (1993).
61. M. Y. Su, J. C. Jao, O. Nalcioglu, Measurement of vascular volume fraction and blood tissue permeability constants with a pharmacokinetic model: studies of rat msucle tumors with dynamic Gd-DTPA enhanced MRI. *Magn. Reson. Med.* **32,** 714–724 (1994).
62. D. M. Shames, R. Kuwatsuru, V. Vexler, A. Muhler, R. C. Brasch, Measurement of capillary permeability to macromolecules by dynamic resonance imaging: a quantitative noninvasive technique. *Magn. Reson. Med.* **29,** 616–22 (1993).
63. P. S. Tofts, B. Berkowitz, M. D. Schnall, Quantitative analysis of dynamic Gd-DTPA enhancement of breat tumors using a permeability model. *Magn. Reson. Med.* **33,** 564–568 (1995).